EPJ Web of Conferences **245**, 06034 (2020) https://doi.org/10.1051/epjconf/202024506034
CHEP 2019

The computational challenge of lattice chiral symmetry

Is it worth the expense?

Adam Virgili[1,*], *Waseem* Kamleh[1,**], and *Derek* Leinweber[1,***]

[1]Special Research Centre for the Subatomic Structure of Matter, Department of Physics, University of Adelaide, South Australia 5005, Australia

Abstract. The origin of the low-lying position of the Roper resonance in the nucleon energy spectrum has been the subject of significant interest for many years, including several investigations using lattice QCD. It has been claimed that chiral symmetry plays an important role in our understanding of this resonance. We present results from our systematic examination of the potential role of chiral symmetry in the low-lying nucleon spectrum through the direct comparison of the clover and overlap fermion actions. After a brief summary of the background motivation, we specify the computational details of the study and outline our comparison methodologies. We do not find any evidence supporting the claim that chiral symmetry plays a significant role in understanding the Roper resonance on the lattice.

1 Introduction

Discovered in 1964 via a partial wave analysis of pion-nucleon scattering data [1], the Roper resonance ($N(1440)\frac{1}{2}^+$) has an unusually large full width of ≈350 MeV [2] and is the lowest-lying resonance in the nucleon spectrum, sitting below the first negative-parity $N(1535)\frac{1}{2}^-$ state. This is a reversal of the ordering predicted by simple quark models.

The nature of the Roper resonance has long been a source of puzzlement. Groups employing correlation matrix analyses in lattice QCD see a quark-model-like radial excitation [3] with a large mass for the first positive-parity excitation, which sits high relative to the Roper resonance, and above the first negative-parity excitation [4–13]. Figure 1 illustrates the agreement among calculations employing local 3-quark operators. However, the χQCD Collaboration have seen a low mass, consistent with the Roper resonance. They emphasise their use of a lattice fermion action which respects chiral symmetry as being key to obtaining their result [14, 15]. It is important to note that the χQCD result is also dependent on their use of the sequential empirical Bayes (SEB) analysis method [16].

We see in Fig. 4 of Ref. [14] that when the SEB algorithm is applied to the same correlation functions, produced with a lattice fermion action which does not respect chiral symmetry, the SEB analysis obtains a ground state mass in agreement with a correlation matrix analysis, but a lower first excited state mass. Our focus, however, is on the apparent ∼300 MeV difference in the first excited state obtained when applying SEB in conjunction with a lattice

*e-mail: adam.virgili@adelaide.edu.au
**e-mail: waseem.kamleh@adelaide.edu.au
***e-mail: derek.leinweber@adelaide.edu.au

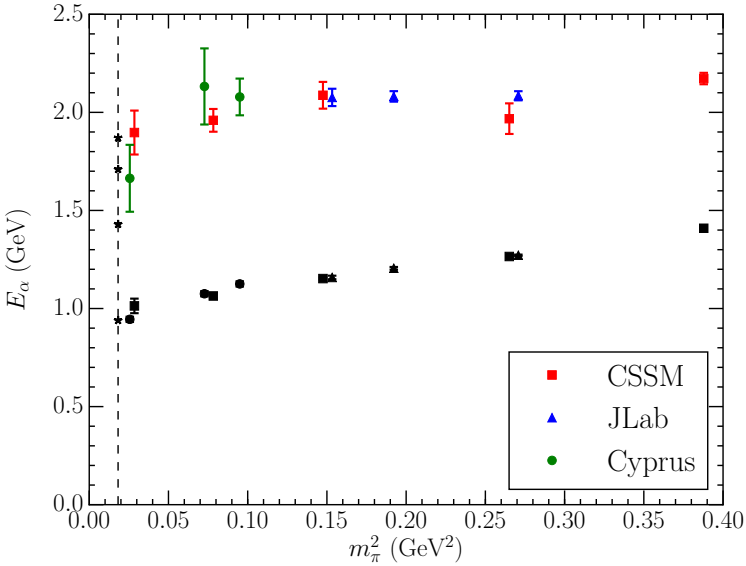

Figure 1. The positive-parity nucleon spectrum obtained from variational analyses employing nonchiral fermions from CSSM [5], JLab [11] and Cyprus [9]. The coloured points are the first excited state masses and the black points are the corresponding ground state masses. The star points correspond to the spectrum observed in nature. The blue JLab point at $m_\pi^2 \approx 0.15$ corresponds to the green point in Fig. 4 of Ref. [14].

fermion action which respects chiral symmetry, in comparison to a fermion action which does not.

Given these discrepancies, we aim to carefully assess the role chiral symmetry plays in understanding the Roper resonance on the lattice.

2 Fermions on the Lattice

There is a great deal of flexibility in how QCD is implemented on the lattice, provided that continuum QCD is recovered in the limit where the lattice spacing $a \to 0$ and the lattice volume $V \to \infty$. Here, we focus on the implementation of fermions.

The implementation of a naive finite-difference discretisation of the fermion action on the lattice results in the phenomenon of fermion doubling whereby we are left with sixteen times the number of fermion species in the continuum limit. This phenomenon can be resolved by the introduction of the $O(a)$ Wilson term to the action [17]. Further modifications to the action yield improved Wilson-type fermions including clover [18] and twisted mass [19] fermions. This does not come without cost, as the Wilson term explicitly violates chiral symmetry for massless fermions. It is then pertinent to ask why we simply do not just find an action which removes doublers whilst preserving chiral symmetry? It turns out it is not straightforward.

The Nielson-Ninomiya no-go theorem [20–22] states that it is not possible to find a local, doubler-free, lattice Dirac operator which obeys chiral symmetry, and has the correct continuum limit. A means to circumvent the powerful no-go theorem was formulated in 1982 in the Ginsparg-Wilson relation [23]

$$\{D, \gamma^5\} = 2aD\gamma^5 D\,, \tag{1}$$

where D is some lattice Dirac operator, which defines a lattice deformed version of chiral symmetry. Initially thought to be inconsequential as there was no known solution, one was eventually found in the form of the overlap Dirac operator [24–29].

The overlap Dirac operator D_{o} is defined by

$$D_{\mathrm{o}} = \frac{1}{2}\left(1 + \gamma_5 \epsilon(H)\right) , \tag{2}$$

where $\epsilon(H)$ is the matrix sign function, and typically $H = \gamma^5 D_{\mathrm{w}}$, the Hermitian form of the Wilson-Dirac operator. As the matrix sign function is expensive to evaluate, simulations which employ overlap fermions are on the order of 100 times more computationally expensive than those which use Wilson-type fermions.

3 NP improved clover versus overlap valence fermions

The role that chiral symmetry plays in understanding the Roper resonance on the lattice can be assessed through the direct comparison of results obtained from simulations employing nonchiral and chiral fermions, respectively. We choose to compare results obtained using the chiral symmetry breaking nonperturbatively (NP) improved clover action [18] to those obtained using the overlap action with $H = D_{\mathrm{flic}}$, where D_{flic} is the fat-link irrelevant clover (FLIC) fermion action [30, 31]. Specifically, we seek to determine if the chiral symmetry preserving overlap fermion action delivers a finite-volume spectrum 300 MeV lower than the NP improved clover action.

The respective simulations are carried out on PACS-CS 2 + 1-flavour configurations [32] at $m_\pi = 0.3881(16)$ GeV. To ensure that any differences in the results are due to choice of fermion action all analysis techniques are matched. We ensure the set of gauge fields used, correlation matrix construction, smearing parameters, and variational parameters are identical across both simulations. Simulations are performed at three valence quark masses corresponding to $m_\pi = 0.435(4)$, $0.577(4)$, and $0.698(4)$ GeV, tuned to match for both actions.

3.1 Variational correlation matrix analysis

To extract states we employ variational correlation matrix analyses [33, 34]. We construct the matrix of Euclidean time cross correlation functions for momentum $\vec{p}$

$$\mathcal{G}_{ij}(\vec{p}, t) = \sum_{\vec{x}} \mathrm{e}^{-i\vec{p}\cdot\vec{x}} \left\langle\, \Omega \left| \chi_i(\vec{x}, t) \overline{\chi}_j(\vec{0}, t_{src}) \right| \Omega \,\right\rangle , \tag{3}$$

where $\overline{\chi}_j$ and χ_i are the respective baryon creation and annihilation operators carrying the quantum numbers of the nucleon, t_{src} is the source creation time, and t is the sink annihilation time. Dirac-traced correlation functions $G_{ij}(\vec{p},\, t)$ at $\vec{p} = \vec{0}$ are

$$G_{ij}(t) = \mathrm{Tr}\left[\Gamma_{\pm}\, \mathcal{G}_{ij}(\vec{p} = 0,\, t)\right] , \tag{4}$$

where the parity projection operator $\Gamma_{\pm} = \frac{1}{2}\left(\gamma_0 \pm I\right)$ projects out positive/negative parity. Introducing a complete set of states, $I = \sum_\alpha \left|\, \alpha \,\right\rangle\!\left\langle\, \alpha \,\right|$, into Eq. (3) we can write

$$G_{ij}(t) = \sum_{\alpha} \lambda_i^{\alpha}\, \bar{\lambda}_j^{\alpha}\, \mathrm{e}^{-m_\alpha t} , \tag{5}$$

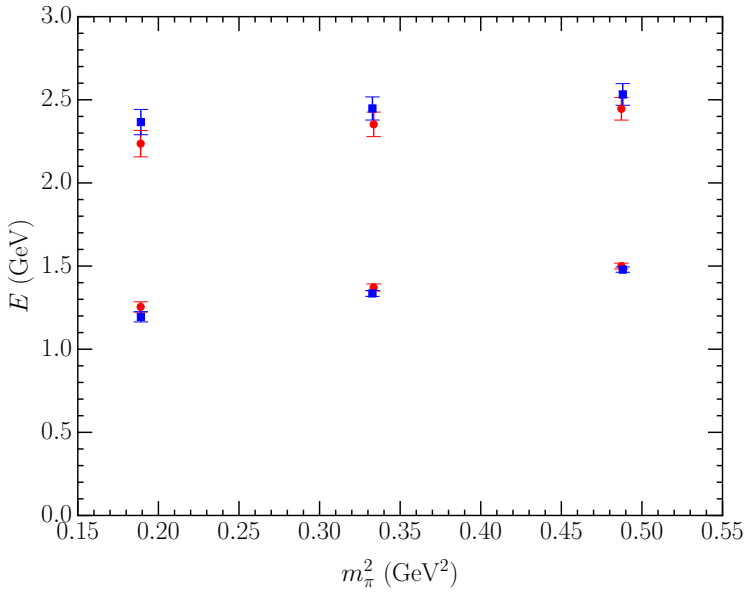

Figure 2. Nucleon ground and first excited state masses for clover (blue, square) and overlap (red, circle) actions as a function of m_π^2.

where m_α is the mass of the αth energy eigenstate, $\lambda_i^\alpha = \langle\, \Omega \,|\chi_i|\, \alpha \,\rangle$ and $\bar{\lambda}_j^\alpha = \langle\, \alpha \,|\bar{\chi}_j|\, \Omega \,\rangle$. We search for a linear combination of the creation and annihilation operators

$$\bar{\phi}^\alpha = \bar{\chi}_j\, u_j^\alpha \qquad \text{and} \qquad \phi^\alpha = \chi_i\, v_i^\alpha\,, \tag{6}$$

which ideally couple to a single energy eigenstate. In practice, the energies observed in lattice QCD calculations can be contaminated with states not captured by the span of the basis of operators. To minimise this effect, improved analysis techniques have been developed [7]. From Eq. (5) we can find u_j^α and v_i^α for a choice of variational parameters t_0 and dt by solving

$$\left[G^{-1}(t_0)\, G(t_0 + dt)\right]_{ij} u_j^\alpha = e^{-m_\alpha\, dt}\, u_i^\alpha\,, \tag{7}$$

and

$$v_i^\alpha \left[G(t_0 + dt)\, G^{-1}(t_0)\right]_{ij} = e^{-m_\alpha\, dt}\, v_j^\alpha\,, \tag{8}$$

the left- and right-handed eigenvalue equations, to obtain the eigenstate projected correlator

$$G^\alpha(t) = v_i^\alpha\, G_{ij}(t)\, u_j^\alpha\,. \tag{9}$$

The spectrum obtained from our analysis is presented in Fig. 2 for variational parameters $t_0 = 1$ relative to the source at $t_{src} = 0$ and $t = t_0 + dt = 4$. All corresponding masses are in statistical agreement across both actions.

3.2 Direct comparison of projected correlators

The results presented in Fig. 2 are dependent on specific choices of fit windows. To improve the robustness of our results, we investigate further, avoiding the selection of fit windows.

First, we consider the projected correlator for the αth energy eigenstate

$$G^{\alpha}(t) \sim e^{-m_{\alpha}t}\,, \tag{10}$$

obtained from our variational analysis and compute the effective mass function

$$M^{\alpha}_{\text{eff}}(t) = \ln\left(\frac{G^{\alpha}(t)}{G^{\alpha}(t+1)}\right). \tag{11}$$

Initially calculating the ratio of the first excited and ground state effective mass functions, respectively for each action

$$R_{1/0}(t) = M^{1}_{\text{eff}}(t)/M^{0}_{\text{eff}}(t)\,, \tag{12}$$

we then take the ratio of these ratios

$$\mathcal{R}(t) = \frac{R^{\text{clover}}_{1/0}(t)}{R^{\text{overlap}}_{1/0}(t)}, \tag{13}$$

providing a comparison of the ratio of the two masses from each fermion action.

Secondly, we again begin with the projected correlator for the αth energy eigenstate from Eq. (10), this time calculating the effective mass splitting between the first excited and ground states for each action, respectively, by taking the ratio of correlators

$$G_{1/0}(t) = G^{1}(t)/G^{0}(t)\,, \tag{14}$$

and applying the effective mass function

$$\Delta M_{\text{eff}}(t) = \ln\left(\frac{G_{1/0}(t)}{G_{1/0}(t+1)}\right). \tag{15}$$

We then take the difference

$$\mathcal{D}(t) = \Delta M^{\text{clover}}_{\text{eff}}(t) - \Delta M^{\text{overlap}}_{\text{eff}}(t) \tag{16}$$

corresponding to the difference between the mass splittings of each action in GeV.

We present results for $\mathcal{R}(t)$ and $\mathcal{D}(t)$ for a variety of variational parameters in Figs. 3, 4, 5, and 6. In each case we compute the χ^2/d.o.f. for fits of $\mathcal{R}(t)$ and $\mathcal{D}(t)$ to constants one and zero, respectively for $2 \leqslant t \leqslant 6$ which are presented in Tables 1, 2, 3, and 4. We note that $\mathcal{R}(t) = 1$ and $\mathcal{D}(t) = 0$ correspond to no difference in excitation energies between the actions.

4 In Summary

We have systematically compared results obtained from simulations employing chiral overlap and nonchiral clover fermion actions. The only difference in the calculations is the choice of fermion action. All corresponding masses are in statistical agreement across both actions. Both the ratio $\mathcal{R}(t)$ of the respective first excited to ground state effective mass ratios and the difference $\mathcal{D}(t)$ of the mass splittings are statistically consistent with no difference in excitation energies produced by each action for a range of variational parameters. We find no evidence that chiral symmetry plays a significant role in understanding the Roper resonance on the lattice. Hence, the implementation of chiral symmetry on the lattice is not worth the additional computational expense when studying the nucleon spectrum.

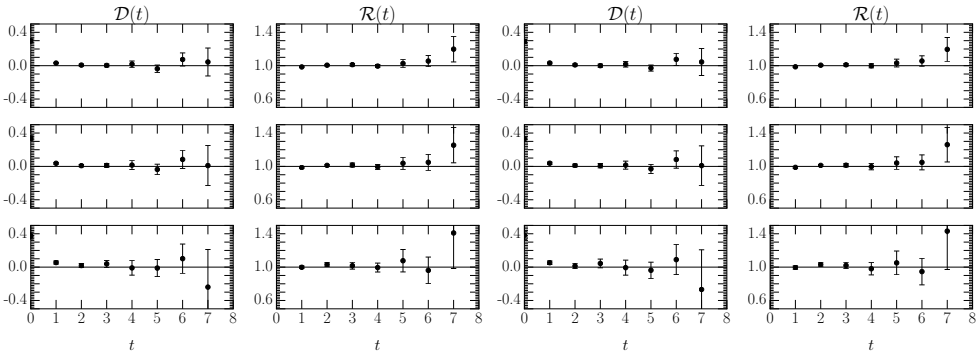

Figure 3. $\mathcal{D}(t)$ and $\mathcal{R}(t)$ at three different pion masses with $m_\pi = 0.698(4)$ GeV (top); $m_\pi = 0.577(4)$ GeV (middle); and $m_\pi = 0.435(4)$ GeV (bottom), for variational parameters $t_0 = 1$ and $t = t_0 + dt = 4$ with $t_{src} = 0$.

Figure 4. $\mathcal{D}(t)$ and $\mathcal{R}(t)$ at three different pion masses with $m_\pi = 0.698(4)$ GeV (top); $m_\pi = 0.577(4)$ GeV (middle); and $m_\pi = 0.435(4)$ GeV (bottom), for variational parameters $t_0 = 1$ and $t = t_0 + dt = 5$ with $t_{src} = 0$.

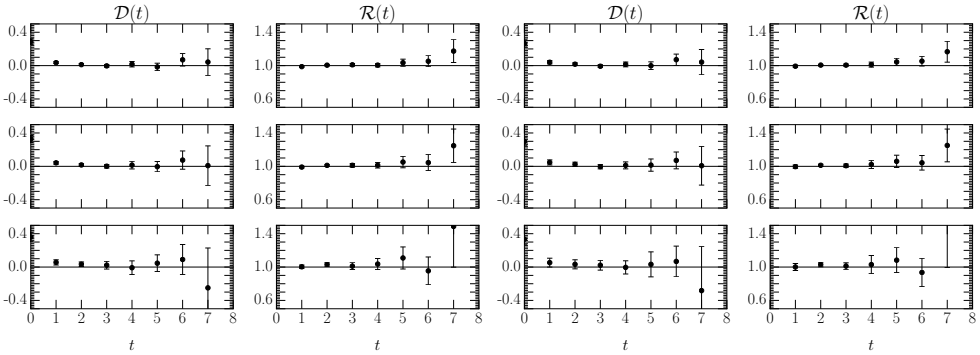

Figure 5. $\mathcal{D}(t)$ and $\mathcal{R}(t)$ at three different pion masses with $m_\pi = 0.698(4)$ GeV (top); $m_\pi = 0.577(4)$ GeV (middle); and $m_\pi = 0.435(4)$ GeV (bottom), for variational parameters $t_0 = 2$ and $t = t_0 + dt = 4$ with $t_{src} = 0$.

Figure 6. $\mathcal{D}(t)$ and $\mathcal{R}(t)$ at three different pion masses with $m_\pi = 0.698(4)$ GeV (top); $m_\pi = 0.577(4)$ GeV (middle); and $m_\pi = 0.435(4)$ GeV (bottom), for variational parameters $t_0 = 2$ and $t = t_0 + dt = 5$ with $t_{src} = 0$.

Table 1. χ^2/d.o.f. for variational parameters $t_0 = 1$ and $t = t_0 + dt = 4$ with $t_{src} = 0$, corresponding to Fig. 3.

m_π/GeV	$\mathcal{D}(t)$	$\mathcal{R}(t)$
0.698(4)	0.842	0.757
0.577(4)	0.595	0.850
0.435(4)	0.619	1.002

Table 2. χ^2/d.o.f. for variational parameters $t_0 = 1$ and $t = t_0 + dt = 5$ with $t_{src} = 0$, corresponding to Fig. 4.

m_π/GeV	$\mathcal{D}(t)$	$\mathcal{R}(t)$
0.698(4)	0.874	0.821
0.577(4)	0.556	0.811
0.435(4)	0.493	0.930

Table 3. χ^2/d.o.f. for variational parameters $t_0 = 2$ and $t = t_0 + dt = 4$ with $t_{src} = 0$, corresponding to Fig. 5.

m_π/GeV	$\mathcal{D}(t)$	$\mathcal{R}(t)$
0.698(4)	0.772	0.804
0.577(4)	0.594	0.841
0.435(4)	0.816	0.962

Table 4. χ^2/d.o.f. for variational parameters $t_0 = 2$ and $t = t_0 + dt = 5$ with $t_{src} = 0$, corresponding to Fig. 6.

m_π/GeV	$\mathcal{D}(t)$	$\mathcal{R}(t)$
0.698(4)	1.032	1.031
0.577(4)	0.728	0.992
0.435(4)	0.528	0.843

Acknowledgments

This research was supported by resources and services provided by the National Computational Infrastructure (NCI) in Canberra, Australia, which is supported by the Australian Government; The Pawsey Supercomputing Centre in Perth, Australia, which is funded by the Australian Government and the Government of Western Australia; and the Phoenix HPC service at the University of Adelaide. This research was supported by the Australian Research Council through ARC Discovery Project Grants Nos. DP150103164, DP190102215, and DP190100297 and ARC Linkage Infrastructure Grant LE190100021.

References

[1] L.D. Roper, Phys. Rev. Lett. **12**, 340 (1964)
[2] M. Tanabashi, K. Hagiwara, K. Hikasa, K. Nakamura, Y. Sumino, F. Takahashi, J. Tanaka, K. Agashe, G. Aielli, C. Amsler et al. (Particle Data Group), Phys. Rev. D **98**, 030001 (2018)
[3] D.S. Roberts, W. Kamleh, D.B. Leinweber, Phys. Rev. **D89**, 074501 (2014), 1311.6626
[4] M.S. Mahbub, W. Kamleh, D.B. Leinweber, P.J. Moran, A.G. Williams (CSSM Lattice), Phys. Lett. **B707**, 389 (2012), 1011.5724
[5] M.S. Mahbub, W. Kamleh, D.B. Leinweber, P.J. Moran, A.G. Williams, Phys. Rev. **D87**, 094506 (2013), 1302.2987
[6] Z.W. Liu, W. Kamleh, D.B. Leinweber, F.M. Stokes, A.W. Thomas, J.J. Wu, Phys. Rev. **D95**, 034034 (2017), 1607.04536
[7] A.L. Kiratidis, W. Kamleh, D.B. Leinweber, B.J. Owen, Phys. Rev. **D91**, 094509 (2015), 1501.07667
[8] A.L. Kiratidis, W. Kamleh, D.B. Leinweber, Z.W. Liu, F.M. Stokes, A.W. Thomas, Phys. Rev. **D95**, 074507 (2017), 1608.03051
[9] C. Alexandrou, T. Leontiou, C.N. Papanicolas, E. Stiliaris, Phys. Rev. **D91**, 014506 (2015), 1411.6765
[10] C.B. Lang, L. Leskovec, M. Padmanath, S. Prelovsek, Phys. Rev. **D95**, 014510 (2017), 1610.01422
[11] R.G. Edwards, J.J. Dudek, D.G. Richards, S.J. Wallace, Phys. Rev. **D84**, 074508 (2011), 1104.5152
[12] R.G. Edwards, N. Mathur, D.G. Richards, S.J. Wallace (Hadron Spectrum), Phys. Rev. **D87**, 054506 (2013), 1212.5236
[13] J.J. Dudek, R.G. Edwards, Phys. Rev. **D85**, 054016 (2012), 1201.2349
[14] K.F. Liu, Y. Chen, M. Gong, R. Sufian, M. Sun, A. Li, PoS **LATTICE2013**, 507 (2014), 1403.6847
[15] K.F. Liu, Int. J. Mod. Phys. **E26**, 1740016 (2017), [,199(2017)], 1609.02572

[16] Y. Chen, S.J. Dong, T. Draper, I. Horvath, K.F. Liu, N. Mathur, S. Tamhankar, C. Srinivasan, F.X. Lee, J.b. Zhang (2004), hep-lat/0405001
[17] K.G. Wilson, Phys. Rev. **D10**, 2445 (1974), [,45(1974); ,319(1974)]
[18] B. Sheikholeslami, R. Wohlert, Nucl. Phys. **B259**, 572 (1985)
[19] R. Frezzotti, P.A. Grassi, S. Sint, P. Weisz (Alpha), JHEP **08**, 058 (2001), hep-lat/0101001
[20] H.B. Nielsen, M. Ninomiya, Nucl. Phys. **B185**, 20 (1981)
[21] H.B. Nielsen, M. Ninomiya, Phys. Lett. **105B**, 219 (1981)
[22] H.B. Nielsen, M. Ninomiya, Nucl. Phys. **B193**, 173 (1981)
[23] P.H. Ginsparg, K.G. Wilson, Phys. Rev. **D25**, 2649 (1982)
[24] R. Narayanan, H. Neuberger, Phys. Lett. **B302**, 62 (1993), hep-lat/9212019
[25] R. Narayanan, H. Neuberger, Nucl. Phys. **B412**, 574 (1994), hep-lat/9307006
[26] R. Narayanan, H. Neuberger, Phys. Rev. Lett. **71**, 3251 (1993), hep-lat/9308011
[27] R. Narayanan, H. Neuberger, Nucl. Phys. **B443**, 305 (1995), hep-th/9411108
[28] H. Neuberger, Phys. Lett. **B417**, 141 (1998), hep-lat/9707022
[29] Y. Kikukawa, H. Neuberger, Nucl. Phys. **B513**, 735 (1998), hep-lat/9707016
[30] W. Kamleh, D.H. Adams, D.B. Leinweber, A.G. Williams, Phys. Rev. **D66**, 014501 (2002), hep-lat/0112041
[31] J.M. Zanotti, S. Bilson-Thompson, F.D.R. Bonnet, P.D. Coddington, D.B. Leinweber, A.G. Williams, J.B. Zhang, W. Melnitchouk, F.X. Lee (CSSM Lattice), Phys. Rev. **D65**, 074507 (2002), hep-lat/0110216
[32] S. Aoki, K.I. Ishikawa, N. Ishizuka, T. Izubuchi, D. Kadoh, K. Kanaya, Y. Kuramashi, Y. Namekawa, M. Okawa, Y. Taniguchi et al. (PACS-CS Collaboration), Phys.Rev. **D79**, 034503 (2009), 0807.1661
[33] C. Michael, Nucl. Phys. **B259**, 58 (1985)
[34] M. Luscher, U. Wolff, Nucl. Phys. **B339**, 222 (1990)